

Electron scattering by vibrationally excited H₂ in the low-energy range

M.-T. Lee

Departamento de Química, UFSCar 13565-905 São Carlos, SP, Brazil

K. T. Mazon

Departamento de Física, UFSCar 13565-905 São Carlos, SP, Brazil

(Received 23 October 2001; published 2 April 2002)

A theoretical investigation on low-energy electron scattering of vibrationally excited H₂ molecules is reported. Cross sections for elastic and inelastic collisional processes calculated for the four lowest-vibrational-state targets are presented in the 1–10-eV energy range. The body-frame vibrational close-coupling approach which accounts for exactly the vibrational effects is used to solve the scattering equations. An optical potential, composed by the exact static-exchange and parameter-free correlation-polarization contributions, is used to represent the collisional dynamics. The calculated integral cross sections for both elastic and $\Delta v = 1$ excitation processes show resonance features for initial states with $v \geq 2$. These structures are associated to the ${}^2\Sigma_u^+$ shape resonance. Also in general, the scattering cross sections for excited targets are larger than those for ground-state target. Their magnitudes at the maxima can be roughly related with the size of the target at each vibrational level.

DOI: 10.1103/PhysRevA.65.042720

PACS number(s): 34.80.Gs

I. INTRODUCTION

Electron-molecule interactions play important roles in a number of applications such as lasers, gas discharges, plasmas, magnetohydrodynamic power generation, etc. [1,2]. Therefore, it is not surprising that the e^- -molecule scattering has been a subject of intense theoretical and experimental investigations during the last three decades [3–6]. In particular, the knowledge of e^- -H₂ scattering cross sections is also important for atmospheric and astrophysical studies, since hydrogen is one of the major constituents of planets, stars, and other celestial objects.

Considering that plasma environments are composed of many species such as electrons, molecules in their ground and excited states, neutral radicals, ionic fragments, etc., the knowledge of cross sections of electron interactions with all these constituents is important for plasma modeling. Specifically, the cross sections of electron scattering by excited molecules are expected to be much larger than those by the ground-state molecules and thus would contribute significantly to plasma properties. Nevertheless, most experimental works measure solely cross sections for electron collisions with ground-state molecules. Only recently, electron-impact ionization-cross-section measurements for some free radicals have been reported [7–9]. Electron collisions with excited atomic targets are also available [10]. For molecular targets, only limited experimental studies on electron scattering by vibrationally excited CO and CO₂ molecules were reported in the literature [11–13]. Therefore, reliable theoretical calculations are certainly of interest in order to fill this lacuna.

On the theoretical side, despite the significant progress achieved during the last two decades, studies on electron collisions with excited molecules are still very limited. In 1993, Ceriberto and Rescigno [14] studied the dependence of the excitation cross sections for the $X\,{}^1\Sigma_g^+ \rightarrow B\,{}^1\Sigma_u^+$ and $C\,{}^1\Pi_u$ transitions in H₂ on vibrational quantum numbers of the initial state. Satori *et al.* [15] have investigated the elec-

tron scattering by $c\,{}^3\Pi_u$ metastable state of H₂ in the low-incident-energy range.

Specifically for vibrationally excited targets, integral cross sections (ICS's) of the vibrational $\Delta v = 1$ transitions for electron scattering by H₂ ($v = 0, 1, 2$, and 3) were calculated by Robicheaux [16] and Gao [17] in the 1–5-eV energy range using a combination of R -matrix method and the multichannel quantum-defect theory (MQDT). In their studies, a set of Born-Oppenheimer eigenstates of compound $e^- + \text{H}_2$ system was found inside the reactive zone whereas the nonadiatic effects were accounted for through an energy-dependent rovibrational-frame-transformation approach. Their study revealed the high dependence of the $\Delta v = 1$ excitation ICS's on the initial vibrational states. Moreover, some resonance-like structures were seen in the calculated ICS's for the initial vibrational quantum states with $v \geq 2$. The origin of these structures was attributed to the occurrence of the ${}^2\Sigma_u^+$ shape resonance. Unfortunately, the existence of these structures cannot be confirmed for the lack of such experimental investigations. Also, the reason for which these structures appear only for $v \geq 2$ initial vibrational states is still to be understood. Therefore, more theoretical investigations on this matter, particularly those using different approaches, are certainly of interest.

Recently, we reported on a theoretical study of electron-impact vibrational excitation of H₂ in the 1–100-eV range [18]. The body-frame vibrational close-coupling (BFVCC) framework [19,20], which incorporates exactly the coupling of the scattering electron and vibrational motions of the nuclei, was used. An optical potential with exact static-exchange plus parameter-free, correlation-polarization contributions were used to represent the interaction dynamics. Our calculated cross sections for $v = 0 \rightarrow v' = 0, 1, 2$, and 3 vibrational transitions in e^- -H₂ collisions are in good agreement with experimental data available in the literature. In the present work, we extend the study to electron scattering by

low-lying vibrationally excited H_2 at low incident energies. More specifically, vibrationally elastic and inelastic cross sections for e^- - H_2 ($v = 1, 2$, and 3) collisions are reported in the 1–10-eV energy range. The comparison of these data with those from the e^- - H_2 ($v = 0$) scattering as well as with those obtained using the MQDT would provide insights of the interaction dynamics between the projectile electron and excited targets. Additionally, it is also hoped that the results reported in the present study can be useful for applications in plasma modeling and atmospheric and astrophysical studies.

Moreover, the inadequacy of uncorrelated Hartree-Fock (HF) level calculations to provide correct potential-energy curves for diatomic molecules is well known, mainly for large internuclear distances. Therefore, it is expected that the neglect of the target electronic correlation in electron-impact vibrational-excitation studies may cause errors in the calculated cross sections, particularly for vibrationally excited targets. For this reason, the present study made use of both the HF and configuration-interaction (CI) target wave functions. The comparison of the calculated results would provide a quantitative estimate of the influence of electronic correlation effects on electron- H_2 vibrational collisions.

The organization of this paper is the following: in Sec. II, we describe briefly the theory used and also give some details of the calculation. In Sec. III, we compare our calculated results with other theoretical data available in the literature and also summarize our conclusions.

II. THEORY AND CALCULATIONS

The theoretical approaches used here have already been presented elsewhere and thus will only be briefly outlined. The projectile-target collisional dynamics is described by the BFVCC approximation. In this approach, the electronic and nuclear motions of the target are separated using the well-known Born-Oppenheimer approximation while the coupling between the scattered electron and vibrational degree of freedom of the target is treated exactly. This coupling dynamics can be appropriately represented by the BFVCC Lippmann-Schwinger integral equation in the matrix form

$$\tilde{\Psi} = \tilde{S} + \tilde{G}_0 \tilde{U} \tilde{\Psi} \quad (1)$$

where, $\tilde{\Psi}$ is the wave function of the scattering electron in matrix form, \tilde{S} is a diagonal matrix that represents a set of solutions of the unperturbed Schrödinger equation, \tilde{G}_0 is also a diagonal matrix which represents the unperturbed Green's operator, and \tilde{U} is the potential operator matrix with elements $U_{v'v} = \langle v' | U^{int}(\vec{r}, R) | v \rangle$, representing the coupling between the initial vibrational state $|v\rangle$ and the final vibrational state $|v'\rangle$. In the present work, Eq. (1) is solved using the method of continued fractions (MCF) [21–24]. The MCF is a numerical method that solves iteratively the Lippmann-Schwinger scattering equation. When the convergence of iterative procedure is achieved, the calculated reactance matrix \tilde{K} would correspond to the exact solution of Eq. (1). Subsequently, the transition matrix \tilde{T} and the vibrationally elastic

and excitation cross sections can be calculated using the \tilde{K} matrix in a conventional manner [18].

The electron-molecule interaction potential for low-energy vibrational excitation is formed by three main components, viz.,

$$U^{int}(\vec{r}, R) = U^{st}(\vec{r}, R) + U^{cp}(\vec{r}, R) + U^{ex}(\vec{r}, R). \quad (2)$$

The static potential $U^{st}(\vec{r}, R)$, is the electrostatic term arising from Coulomb interactions between the projectile and the nuclei and electrons of the target. In this study, the R -dependent U^{st} was derived exactly from the target wave functions. These were calculated for 15 internuclear distances varying from 0.6 to 3.5 a.u. At each distance, the ground-state target wave function was calculated using both the HF self-consistence-field and CI approximations.

The U^{cp} that appeared in Eq. (2) is the correlation-polarization potential arising at short range from bound-free many-body effects and at long range from induced polarization effects. This contribution is approximated by a parameter-free local potential as prescribed by Padial and Norcross [25]. The R -dependent target wave functions were used to calculate the short-range correlation potentials, whereas the published R -dependent dipole polarizabilities of H_2 [26] were used to describe the asymptotic form of the U^{cp} .

The third term in the right-hand side of Eq. (2) is a non-local energy-dependent exchange contribution arising from the antisymmetric consideration between the scattering and the target electrons. This nonlocal contribution to the transition $|v'\rangle \rightarrow |v\rangle$ was accounted for by using a separable potential approach. A set of one-dimensional particle-in-box wave functions is used as the expansion basis. Details of this approach were already discussed in our previous work [18] and will not be repeated here.

Finally, in order to calculate the vibrational excitation interaction potential matrix elements $U_{v'v}$, the vibrational wave functions $\chi_v(R)$ were calculated using the numerical method of Cooley [27] from the Rydberg-Klein-Rees potential curve of the ground electronic state H_2 [28]. These wave functions were calculated in a 901-point grid, covering the $0.6 \leq R \leq 3.5$ a.u. range. The R -dependent interaction potentials defined in Eq. (2) were interpolated over the same grid and the integral over this internuclear-distance grid was evaluated using the Simpson's rule.

The number of vibrational states that must be included for solving the BFVCC scattering equation depends on the incident energy, especially on whether the scattering is resonant or nonresonant. In the energy range covered herein, six vibrational states were used, which implied the convergence of the reported cross sections to better than 1% for initial vibrational states with $v \leq 2$ and up to 5% for the $v = 3$ initial state.

It is well known that the $(e^- + \text{H}_2) \ ^2\Sigma_u^+$ resonance becomes a true bound state at internuclear distances $R \geq 3.0$ a.u. [16], which can lead to dissociation of the molecule to $\text{H}^- + \text{H}$. In principle, this open reactive channel should also be included in the vibrational close-coupling cal-

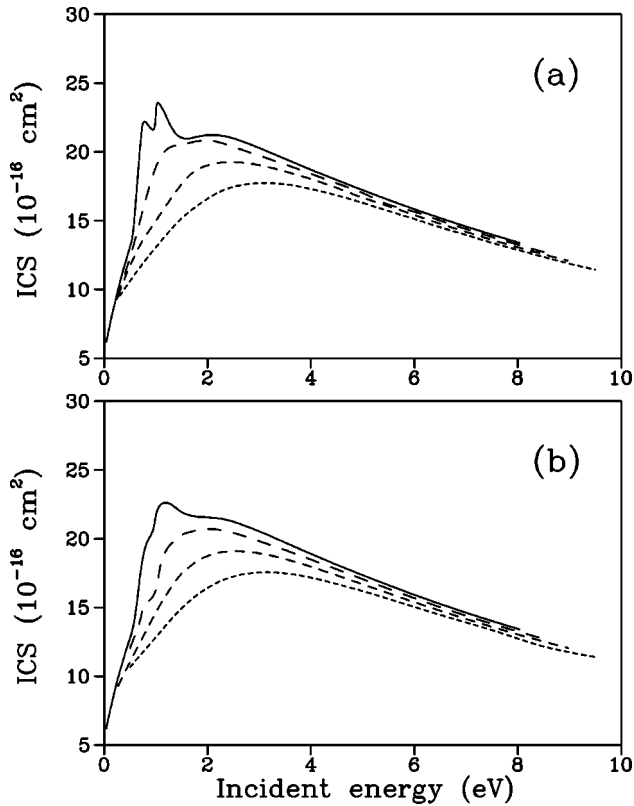


FIG. 1. ICS's for vibrationally elastic electron scattering by H_2 calculated using (a) HF and (b) CI target wave functions. Short-dashed lines for $v=0$ initial vibrational state, dashed line for $v=1$ initial state, long-dashed line for $v=2$ initial state, and solid line for $v=3$ initial state.

culations. However, the highest vibrational state included in the present study is $v=5$, with the larger classic turning point R_{max} located at 2.67 a.u. [28]. Therefore, the density of probability of all vibrational states considered in our calculation should be very small beyond that point. For this reason, the influence of the bound-state formation on the calculated cross sections is expected to be small and thus neglected in the present study. By the way, this statement is also supported by an excellent agreement between the calculated excitation cross sections for vibrational transitions $\Delta v = 1$ in H_2 from the initial states $v \leq 2$ given by Robicheaux [16] and Gao [17]. The bound-state formation effects were explicitly included in the study performed by the first author but neglected by the latter.

III. RESULTS AND DISCUSSIONS

Figures 1(a) and 1(b) show our calculated ICS's using the HF and CI target wave functions, respectively, for the vibrationally elastic electron scattering by H_2 at the four lowest ($v=0, 1, 2$, and 3) vibrational states in the 1–10-eV energy range. In general, there is a good agreement between the calculated HF and CI ICS's, except that some differences are seen for the $v=3 \rightarrow v'=3$ transition at lower end energies. In both the figures, the maximum of the ICS's shifts toward lower incident energies with increasing v . Also, some reso-

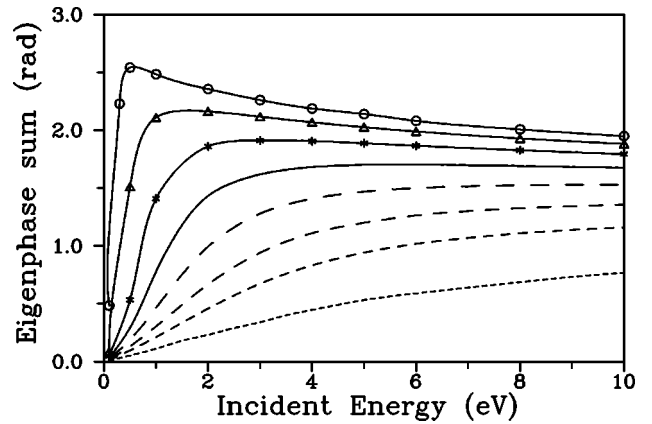


FIG. 2. Fixed-nuclei eigenphase sum for the $^2\Sigma_u^+$ elastic scattering channel in the 1–10-eV range. Dotted line is at $R = 1.0$ a.u., short-dashed line at $R = 1.4006$ a.u., dashed line at $R = 1.6$ a.u., long-dashed line at $R = 1.8$ a.u., solid line with stars at $R = 2.0$ a.u., solid line with open triangles at $R = 2.4$ a.u., and solid line with open circles at $R = 2.6$ a.u.

nancelike structures appear in the ICS's of the target of $v = 3$. In order to understand the nonappearance of resonance features at ICS's of electron scattering by lower-initial-state targets, we present in Fig. 2 the partial eigenphase sum for the $^2\Sigma_u^+$ scattering symmetry, calculated at several fixed internuclear distances R using the CI wave function. One verifies that typical characteristics of shape resonance (sudden increase of eigenphase sums with the energy) begin to show up at around $R = 1.8$ a.u. These characteristics are strongly enhanced for $R \geq 2.2$, where a maximum is located in the probability density distribution of the $v = 3$ vibrational state of H_2 . In contrast, the probability densities of lower vibrational states at this region are small and thus no resonant features appear in their corresponding ICS's.

From Fig. 1, one also sees that the ICS's of electron scattering by the vibrationally excited targets are significantly larger than those by the ground-state target at the lower end energies. At the maxima, the calculated CI (HF) ICS's for the electron scattering by the excited targets with $v = 1, 2$, and 3 are approximately 9% (9%), 19% (18%), and 29% (33%), respectively, which are larger than those for the $v = 0$ target. On the other hand, for incident energies equal to or above 4 eV, all the calculated ICS's are quite similar. Probably, the larger elastic ICS's of excited targets at lower incident energies are related to the occurrence of the $^2\Sigma_u^+$ shape resonance that becomes much more pronounced for higher vibrational states. On the other hand, it is also interesting to note that this increase of the ICS's can be roughly related to the size of the target of different vibrational level. Here we consider that the molecular size (area) of each vibrational level is proportional to the square of its mean internuclear distance (R_v), which is taken as an average of the classical vibrational turning points (R_{min} and R_{max}), as listed in Table I for the four lowest vibrational levels of H_2 . It is verified that the ratios of the square of the mean internuclear distances $[R_v/R_0]^2$ for $v = 1, 2$, and 3 are 1.09, 1.18, and 1.29, respectively, and thus are in good agreement with the ratios of the

TABLE I. Some information on the four lowest vibrational states of H_2 .

v	R_{min} (a.u.)	R_{max} (a.u.)	R_v (a.u.)	$[R_v/R_0]^2$
0	1.1968 ^a	1.6675	1.4322	1.000
1	1.0783	1.9147	1.4965	1.092
2	1.0101	2.1163	1.5632	1.191
3	0.9613	2.3038	1.6326	1.299

^aValues taken from Ref. [28].

calculated ICS's (ICS_v/ICS_0) at the maxima. A plot of ICS_v/ICS_0 , calculated using the CI target wave function, at the maxima versus $[R_v/R_0]^2$ is shown in Fig. 3. A very good fitting of a linear function is seen. At higher incident energies, it is expected that the incident electrons can penetrate into the target and thus the size of the molecule becomes less important.

In Figs. 4(a) and 4(b) we present our calculated CI differential cross sections (DCS's) for the vibrationally elastic electron scattering by H_2 at the four lowest vibrational states at 2.5 eV and 7.5 eV, respectively. At 2.5 eV, the minimum for the $v=0 \rightarrow v'=0$ DCS's at around 75° is shifted toward the larger scattering angles with the increasing v . However, at 7.5 eV, the DCS's for electron scattering by targets of different vibrational levels show agreement with each other both qualitatively and quantitatively.

Figures 5(a) and 5(b) show the calculated vibrational excitation ICS's, calculated using the HF and CI target wave functions, respectively, for $\Delta v = +1$ transitions of H_2 with initial states $v=0, 1$, and 2 in the 1–10-eV energy range. The corresponding MQDT data of Gao [17] in the 1–5-eV range are also shown for comparison. Similar to the elastic processes, no resonance features were seen in the vibrational excitation ICS's for the $v=0 \rightarrow v'=1$ and $v=1 \rightarrow v'=2$ transitions, but they do show up in the ICS's for the $v=2 \rightarrow v'=3$ transition. The physical origin of these structures is the same as in elastic scatterings. In general, our calculated results using the CI wave function are in very good agree-

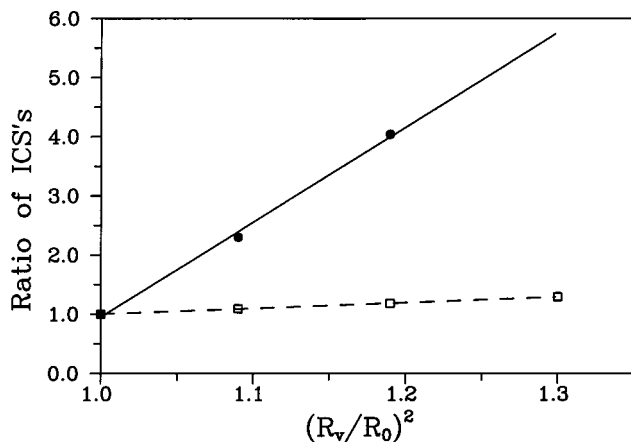


FIG. 3. The ratio ICS_v/ICS_0 versus $[R_v/R_0]^2$. Dashed line with open squares is for vibrationally elastic scattering and solid line with full circles for the $\Delta v = 1$ vibrational transitions.

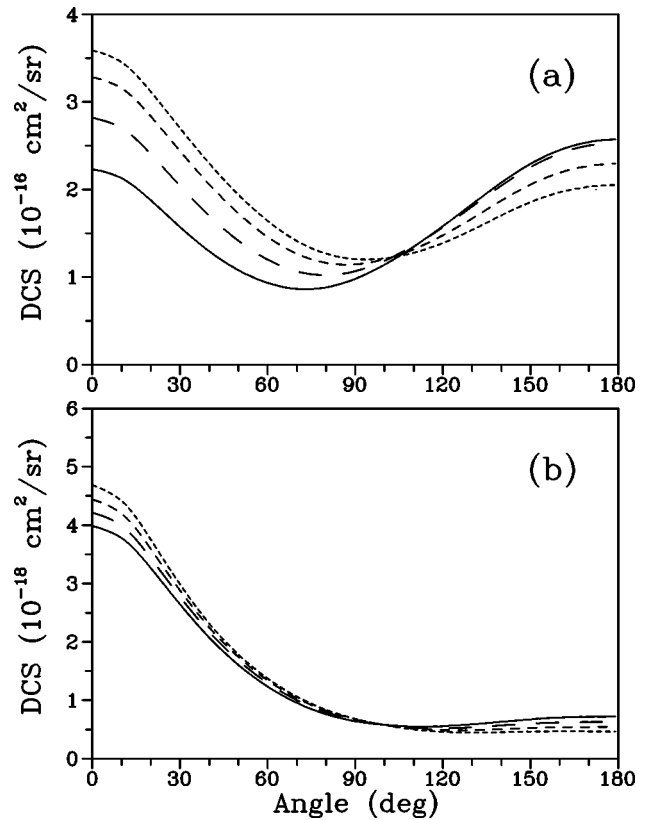


FIG. 4. DCS's for vibrationally elastic e^-H_2 collisions at (a) 2.5 eV and (b) 7.5 eV incident energies. Solid line, is for $v=0$ initial state, long dashed line for $v=1$ initial state, dashed line for $v=2$ initial state, and short-dashed line for $v=3$ initial state.

ment with the MQDT data of Gao in the entire energy range where the comparison is made. Compared to the elastic processes, the dependence of the vibrational excitation ICS's on target initial vibrational states are even more sensitive. At the maxima, ICS's of the $v=1 \rightarrow v'=2$ and $v=2 \rightarrow v'=3$ transitions are larger by multiplicative factors of approximately 2.29 and 4.04, respectively, than those of the $v=0 \rightarrow v'=1$ transition. These values are significantly larger than the ratios $[R_v/R_0]^2$ shown in Table I. However, a plot of ICS_v/ICS_0 at the maxima for $\Delta v = +1$ transitions versus $[R_v/R_0]^2$, also shown in Fig. 3, has revealed a very good fitting of a linear function, which seems to indicate that the vibrational excitation cross sections are somehow also related to the size of the target.

In Figs. 6(a) and 6(b) we present our calculated CI DCS's for the vibrational excitation $\Delta v = +1$ for electron scattering by H_2 at the three lowest vibrational states at 2.5 eV and 8 eV, respectively. For both the incident energies, the DCS's for electron scattering by the targets of different vibrational levels show a qualitative agreement with each other. Quantitatively, even at 8 eV, the magnitude of the DCS's increase with increasing initial v .

In summary, the present work reports a theoretical investigation on low-energy electron scattering by vibrationally excited H_2 . Vibrationally elastic and inelastic ($\Delta v = 1$) cross sections were calculated within the BFVCC framework, using both the HF and CI target wave functions, in the

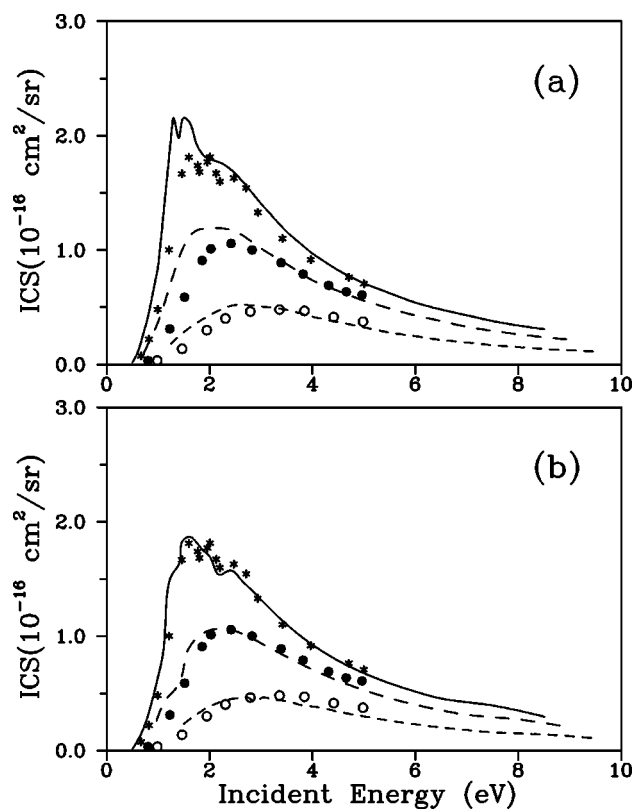


FIG. 5. ICS's for the $\Delta v=1$ vibrational excitation of H_2 by electron impact using (a) HF and (b) CI target wave functions. Short-dashed line is for the $v=0$ initial vibrational state, dashed line for $v=1$ initial state, solid line for $v=2$ initial state and open circles, full circles, and stars represent the calculated results of Gao [17] for the $v=0$, $v=1$, and $v=2$ initial vibrational states, respectively.

1–10-eV energy range. Our study not only confirms the resonance structures seen in the vibrational excitation ($\Delta v=1$) ICS's of Gao for $v \geq 2$ initial states but also predicts the existence of similar structures in the ICS's of elastic electron scattering by excited targets with $v \geq 3$. The origin of these features are also discussed. On the other hand, this study reveals that the effects of target electronic correlation are small for both elastic and inelastic ($\Delta v=1$) scattering of electrons by low-lying vibrationally excited H_2 . Only at incident energies below 3 eV, some differences in the calculated HF and CI ICS's are seen. Particularly, the resonance structures are more visible in the HF ICS's.

For vibrationally elastic processes, our study also shows that at the lower end energies, the calculated cross sections

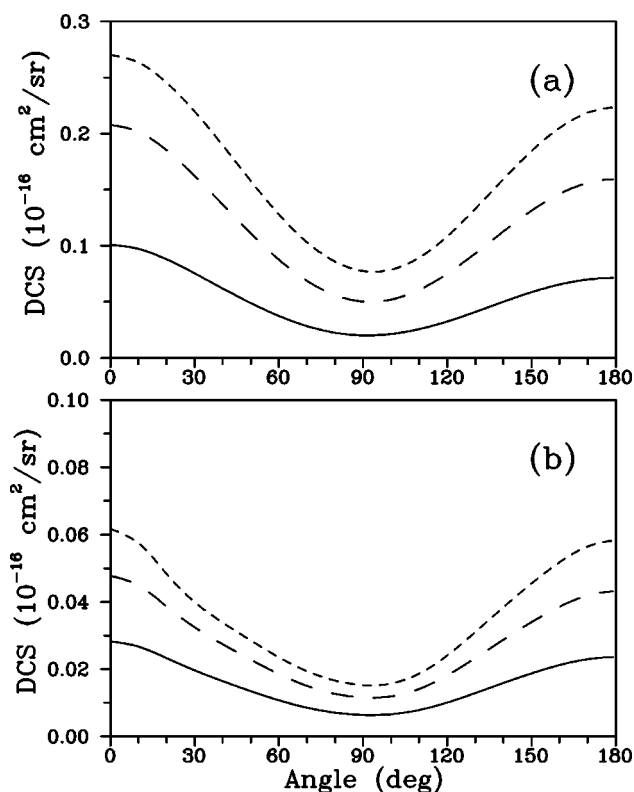


FIG. 6. DCS's for the $\Delta v=1$ vibrational excitation at (a) 2.5 eV and (b) 8 eV incident energies. Solid line is for $v=0$ initial state, long-dashed line for $v=1$ initial state and the dashed line for $v=2$ initial state.

increase with increasing initial vibrational quantum number v . The larger cross sections for excited targets are closely related with the occurrence of the $^2\Sigma_u^+$ shape resonance. But it is interesting to note that they are somehow also related to the size of the targets. At high incident energies, the calculated cross sections for targets of various vibrational states are quite similar, probably due to higher penetration of scattering electrons. For vibrational ($\Delta v=+1$) excitation processes, our calculated CI ICS's are in good agreement with the MQDT data of Gao, both qualitatively and quantitatively, since the MQDT and BFVCC are two very different theoretical approaches. This good agreement is meaningful and indicates the reliability of both the calculated results.

ACKNOWLEDGMENTS

This research was partially supported by the Brazilian agencies FAPESP, CNPq, and FINEP-PADCT. K.T.M. thanks the CAPES for financial support.

- [1] J. Hahn and C. Junge, *Z. Naturforsch. A* **32A**, 190 (1977).
- [2] W. Wang and N.D. Sze, *Nature (London)* **286**, 589 (1980).
- [3] I. Shimamura, *Sci. Pap. Inst. Phys. Chem. Res. (Jpn.)* **82**, 1 (1989).
- [4] L.W. Morgan, *Plasma Chem. Plasma Process.* **12**, 449 (1992).
- [5] A. Zecca, G.P. Karwasz, and R.S. Brusa, *Riv. Nuovo Cimento*

- 19**, 1 (1996).
- [6] G.P. Karwasz, R.S. Brusa, and A. Zecca, *Riv. Nuovo Cimento* **24**, 1 (2001).
- [7] V. Tarnovsky, A. Levin, H. Deutsch, and K. Becher, *J. Phys. B* **29**, 139 (1996).
- [8] C. Tian and C.R. Vidal, *J. Phys. B* **31**, 895 (1998).

- [9] V. Tarnovsky, A. Levin, H. Deutsch, and K. Becher, *J. Chem. Phys.* **109**, 932 (1998).
- [10] P.W. Zetner, S. Trajmar, I. Kanik, S. Wang, G. Csanak, R.E.H. Clark, J. Abdallah, Jr., D. Fursa, and I. Bray, *J. Phys. B* **32**, 5123 (1999).
- [11] J. Michejda, *Bull. Am. Phys. Soc.* **23**, 147 (1978).
- [12] A. Ernesti and H.J. Korsch, *Phys. Rev. A* **44**, R4095 (1991).
- [13] M.W. Johnstone, N.J. Mason, and R.W. Newell, *J. Phys. B* **26**, L147 (1993).
- [14] R. Ceriberto and T.N. Rescigno, *Phys. Rev. A* **47**, 1939 (1993).
- [15] C. Satori, F.J. da Paixão, and M.A.P. Lima, *Phys. Rev. A* **55**, 3243 (1997).
- [16] F. Robicheaux, *Phys. Rev. A* **43**, 5946 (1991).
- [17] H. Gao, *Phys. Rev. A* **45**, 6895 (1993).
- [18] K.T. Mazon, R. Fujiwara, and M.-T. Lee, *Phys. Rev. A* **64**, 042705 (2001).
- [19] N. Chandra and A. Temkin, *Phys. Rev. A* **13**, 188 (1976).
- [20] M.A. Morrison, A.N. Feldt, and D. Austin, *Phys. Rev. A* **29**, 2518 (1984).
- [21] J. Horáček and T. Sasakawa, *Phys. Rev. A* **28**, 2151 (1983).
- [22] M.-T. Lee, M.M. Fujimoto, and I. Iga, *J. Mol. Struct.: THEOCHEM* **432**, 197 (1998).
- [23] M.-T. Lee, M.M. Fujimoto, T. Kroin, and I. Iga, *J. Phys. B* **29**, L425 (1996).
- [24] A.M. Machado, M.M. Fujimoto, A.M.A. Taveira, L.M. Brescansin, and M.-T. Lee, *Phys. Rev. A* **63**, 032707 (2001).
- [25] N.T. Padial and D.W. Norcross, *Phys. Rev. A* **29**, 1742 (1984).
- [26] M.A. Morrison and B.C. Saha, *Phys. Rev. A* **34**, 2786 (1986).
- [27] J.W. Cooley, *Math. Comput.* **15**, 363 (1961).
- [28] R.J. Spindeler, Jr., *J. Quant. Spectrosc. Radiat. Transf.* **9**, 597 (1969).